Supplemental Document

Optics Letters

Deep learning approach for inverse design of metasurfaces with a wider shape gamut: supplement

Soumyashree S. Panda,[1] Sumit Choudhary,[2] Siddharth Joshi,[1] Satinder K. Sharma,[2] and Ravi S. Hegde[1,*]

[1]*Electrical Engineering Discipline, Indian Institute of Technology, Gandhinagar, 382355, India*
[2]*School of Computing and Electrical Engineering, Indian Institute of Technology, Mandi, 175005, India*
[*]*Corresponding author:* *hegder@iitgn.ac.in*

Supplement DOI: https://doi.org/10.6084/m9.figshare.19673781

Parent Article DOI: https://doi.org/10.1364/OL.458746

Supporting document: A Deep Learning approach for inverse design of metasurfaces with a wider shape gamut

SOUMYASHREE S. PANDA[1], SUMIT CHOUDHARY[2], SIDDHARTH JOSHI[1], SATINDER K. SHARMA[2], AND RAVI S. HEGDE[1*]

[1] School of Electrical Engineering, Indian Institute of Technology, Gandhinagar, India, 382355.
[2] School of Computing and Electrical Engineering, Indian Institute of Technology, Mandi, India, 175005.
[*] Corresponding author: hegder@iitgn.ac.in

Compiled April 21, 2022

http://dx.doi.org/10.1364/ao.XX.XXXXXX

S-1. POLYGONAL ENCODING OF METASURFACE GEOMETRY

The polygon is specified by its vertices in a curvilinear coordinate system in terms of r, α and θ, where r represents the distance from the centre of the unit-cell, α is the angle of the last point. The angles θ depict a point's angle with respect to it's previous point. The angles θ sum up to α, they are chosen according to $\theta_i = \frac{\phi_i}{\sum_{i=1}^{n} \phi_i}\ \alpha$ where ϕ_i are the weights. Thus, the 1D tensor that constitutes of the values of r, ϕ and α define the geometry of the metasurface unit cell. Taking fabrication feasibility into account, the values of r and ϕ are chosen as follows: 25nm $< r_1, r_2, ..., r_n < p/2 - 25$nm, ($p$ = periodicity), $20 < \phi_1, \phi_2, ..., \phi_n < 100$. For 8-fold, 4-fold and 2-fold symmetric structures and asymmetric structures, α values are chosen as 45°, 90°, 180° and 360° respectively. For x-fold symmetric structures, the vertices are folded x-times to define the full polygon. The shapes are processed through a 2D interpolation to smooth the sharp edges as discussed in [1]. For robust designs, the perturbed geometries are also considered using the Taguchi's orthogonal array method as reported in [1].

The task was to minimize the mean square error between the transmission spectrum and the Color Matching Function of the target color. The optimization problem was defined as an optimization problem with solution vector length 2n+1 (n is the number of points defined). For a metasurface unit cell with periodicity of p and with N number of wavelength samples the problem can be mathematically defined as follows.

$$min \quad y = f(\overrightarrow{x}) \tag{1}$$

Here,

$$f(\overrightarrow{x}) = \frac{1}{N} \sum_{\lambda=400nm}^{700nm} [\ S(\lambda) - T(\lambda)\ ]^2, \tag{2}$$

where S is the transmission spectrum of the design and T is the target spectrum. The target spectrum to design color filters is a scaled version of the color matching function (CMF) of target color.

S-2. DNN MODEL

We have taken the help of a Deep Neural Network (DNN) to establish the empirical relationship between the geometrical parameters and correspoinding optical characteristics as shown in **figure S-1A**. The Stanford Stratified Structure Solver (S^4) tool [2] which uses the RCWA technique along with S-matrix algorithm to solve Maxwell's equations in layered periodic structures was used for ground truth generation (determining the optical characteristics of the structures). The networks' training was performed in the Keras deep learning platform with a Tensorflow backend on a workstation with an Intel™ i9–7920X CPU with an NVIDIA™ GeForce GTX 1080 GPU card with 128 GB memory.

For ground truth generation, random samples are selected from the design space with uniform probability distribution (example shown in inset of **figure S-1B**). Once selected, the samples are then labelled with respective transmittance/reflectance spectra. Training

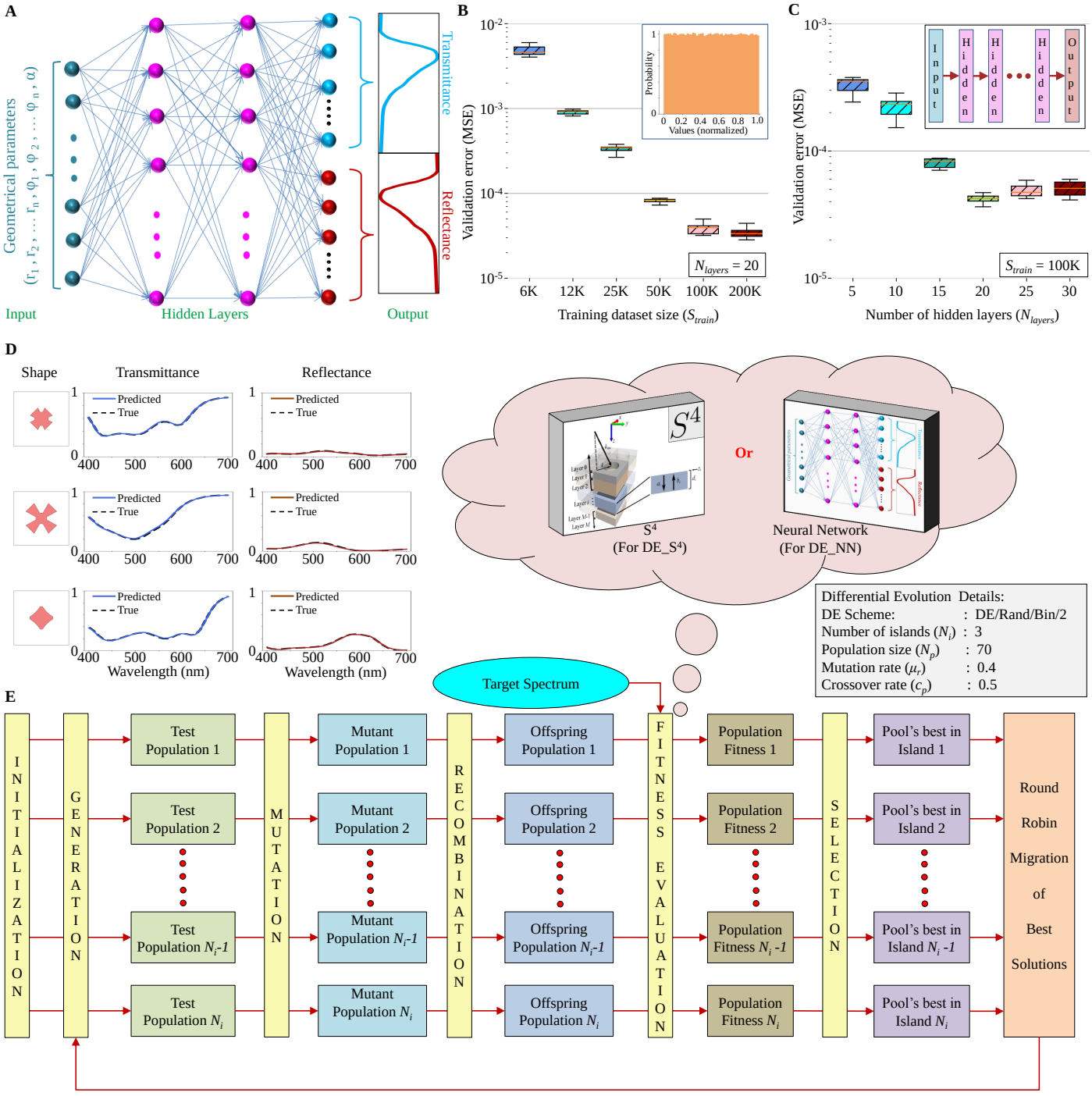

Fig. S-1. Learning model creation and surrogate optimization. **A**: A deep neural network (DNN) model of the structure which predicts the transmitted and reflected power over a wavelength range for a given geometry. Statistical comparison of validation error (MSE) for learning models are shown with **B:** increasing training dataset sizes (inset shows the probability distribution of the training data) and **C:** increasing the number of hidden layers (inset shows the network architecture). **D:** Prediction capability of final learned DNN demonstrated by comparing the true and predicted transmission and reflection spectra of some example structures (geometries given in insets). **E**: Flowchart of a typical DE optimizer with two given choices for function evaluation: (1) Using S^4 for DE_S^4 and (2) DNN model for DE_NN.

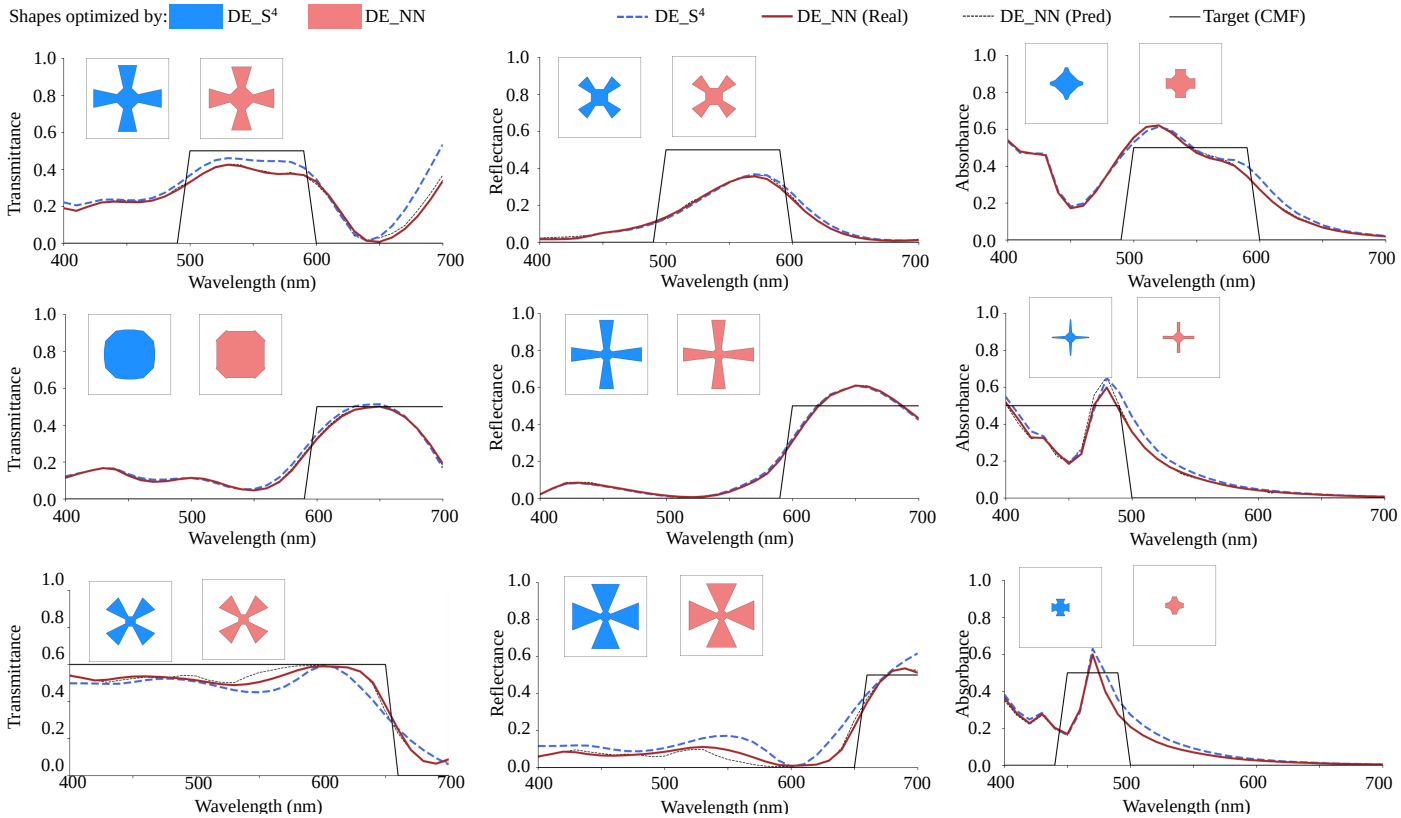

Fig. S-2. Surrogate optimization of polygonal meta-atom geometries for attaining various functionalities. The periodicity of the metasurfaces was kept constant to 380 nm. The results of typical and surrogate optimizations are compared.

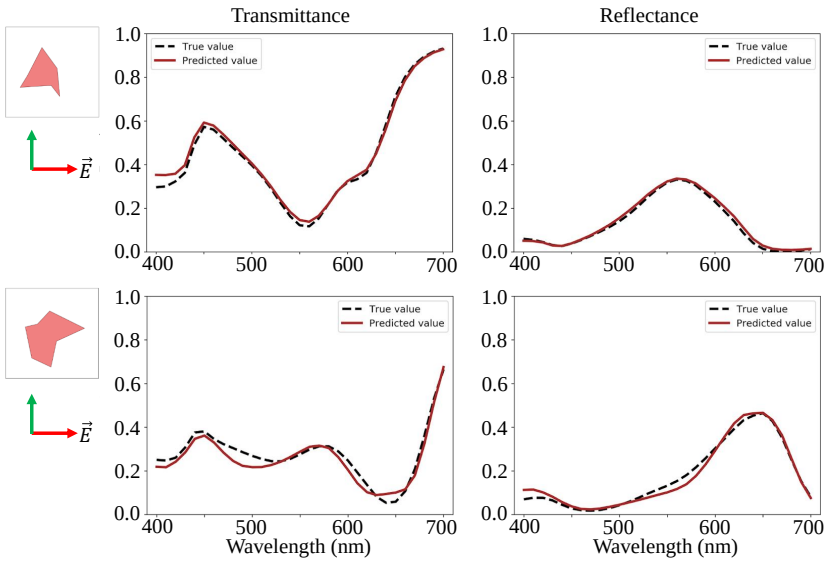

Fig. S-3. Performance of DNN for prediction of higher dimensional geometries. Figure shows the comparison between the actual and DNN-predicted spectra of 7-sided asymmetric polygon (dimensionality of parameter vector = 15) for s-polarized excitation.

datasets of different sizes (S_{train}), starting from 6K and doubling until 200K, are used to train a DNN model. The batch size was fixed to 128 throughout. The experiments were repeated 10 times and the statistical comparison is plotted in **figure S-1C**. It can be observed that the performance (in terms of mean of squared validation error) of the training model saturates for S_{train} more than 100K. Therefore, S_{train} was fixed to 100K for further studies. Unit cell periodicities between 200 nm and 400 nm were discretized with 20 nm spacing. For each of the periodicity, 100K geometries were randomly selected and labelled with their optical characteristics (ground-truth). The S^4 tool was used for the ground truth generation and required ≈50 hours (≈5 hours for each periodicity). The DNN models training takes ≈15 minutes for each periodicity.

A simple feed-forward network architecture with a Sigmoid activation function at the end (shown in insets of **figure S-1C**) was considered for learning. The number of hidden layers (N_{layers}) in the network are increased from 5 to 30 as shown in **figure S-1C**. A performance degradation can be observed after N_{layers} = 20. This performance degradation can be attributed to the vanishing gradient. Thus the number of hidden layers (N_{layers}) are fixed to 20 for rest part of this work. The number of neurons in each layer was fixed to 256 throughout the study. The trained models exhibited a validation error in the order of 1e-5 suggesting near ideal prediction. The predicted and true transmittance and reflectance of some example structures along with the geometry are given in **figure S-1D**. The predicted spectra are observed following the true spectra excellently; suggesting a great prediction ability of the learned model.

S-3. OPTIMIZATION VIA DIFFERENTIAL EVOLUTION (DE)

Differential Evolution (DE) is a stochastic optimization technique that takes a random population as its initial population and performs mutation and crossover in order to produce the next generation solutions [3, 4]. The parent solutions are compared with the offsprings and the solution with best fitness value is promoted for the next generation. The DE used here is an island based technique, where multiple populations are created parallelly and are simultaneously evolved in order to provide a pool of best-fit solution vectors. **Figure S-1E** shows the flow-chart of the island-based DE used for optimization along with details of DE hyperparameters. When the DE optimizer uses the DNN model for function evaluation, it is termed as a surrogate optimization as shown in the flow-chart.

The radii (r), angle weight (ϕ) and maximum angle (α) make a solution vector, which represents an individual. In the optimization of polarization-independent color filters, only 8-fold symmetric structures are considered. As the number of points per octant is kept constant to 3, the length of each solution vector is 7. Each generation consists of N_i number of islands and each island has N_p number of populations. As per convention, the value of N_p is kept between 5 to 10 times of the number of variables (Here between 35 and 70). In each island, the evolution starts from a randomly generated population that are potential solutions to the metasurface design. A test population is also generated in order to compare the fitness with the island's offspring and to take part in the selection process. The target is to match the transmission spectrum of the metasurface with the CMF of a particular color; thus the fitness is the mean square error between the spectrum and the CMF.Each generation has 20 iterations where Mutation, Crossover and Selection takes place. In DE, the mutation takes place first to initiate the genetic diversity in the current pool, then a mutant solution is recombined (Crossed-over) with another solution (that has no part in creating the mutant) in order to generate the offspring. Then best fit solution between parents and offspring is forwarded to the next pool. For both direct and surrogate DE optimizer, the DE schemes used are DE/rand/1/bin for exploration and DE/best/1/bin for exploitation. It was observed that the convergence was fastest when the mutation rate was $m_r = 0.4$ and the crossover probability was $c_p = 0.5$.

Along with the surrogate optimization of transmission-mode RGB and CMY color filter arrays provided in the manuscript, the learned models can be used to optimize metasurface geometries to obtain a wide variety of other target functionalities. As shown in **figure S-2**, a single learned model that learns the transmittance and reflectance of polygonal metasurface with 380 nm lattice can be implemented in the inverse design of a number of transmission, reflection and absorption-mode filters. A great deal of similarity can be observed between DE_S^4 and DE_NN optimized geometries and their respective spectra. The duration of optimization for surrogate DE and typical DE was 100 seconds and 72 minutes respectively. Therefore, the design exploration for multiple functionalities in a single surrogate model can effectively amortize the computational cost invested during the model creation.

The design, simulation and optimization were run in a system with following specifications. Processor : Intel™ i9–7920X; Number of cores: 32, RAM : 128 GB. The solutions satisfied the convergence criteria within 10 generations (20 iterations each).

A. Design for robustness

In order to overcome the fabrication difficulty, the structure that are robust in nature are considered for designing the filters. Robust nanostructures are designed by inducing perturbation errors of ± 10nm for all radius values and preserve the color for all perturbed designs. In order to achieve this, the DE algorithm was used to minimize the variance between spectra obtained by the perturbed structures [1]. Total of perturbed structures are selected with the help of Taguchi's orthogonal array. The objective function considered for optimization to design a robust structure is as follows.

$$f(\overrightarrow{x}) = \eta_1 + \kappa \times \eta_2 \tag{3}$$

Here η_1 is the Mean Squared Difference between the mean of the transmission spectra of all perturbed structures and CMF; η_2 is the cumulative variances of all the perturbed designs from the original structures. A scaling factor κ was multiplied with η_2 in order to keep the objective value of both functions comparable.

B. Prediction of higher dimensional geometries

As the dimensionality of the geometrical parameter vector increases, the solution space explodes exponentially; making inverse design more and more difficult. In such scenario, learned model with good prediction accuracy become more beneficial as they make the design exploration faster. The DNN model proposed in this work can be beneficial in such scenarios.

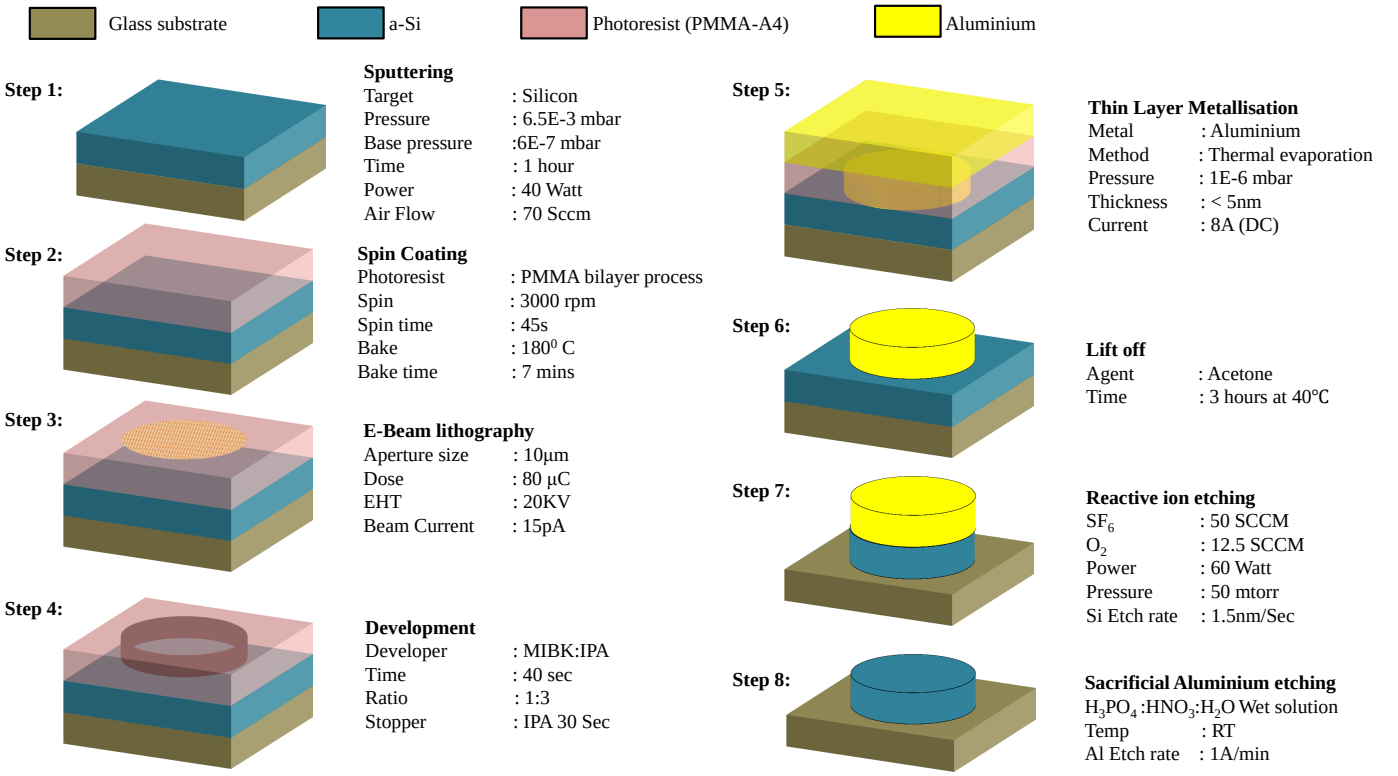

Fig. S-4. Step-by-step details of fabrication process. Parameter values at different junctures of fabrication are also listed.

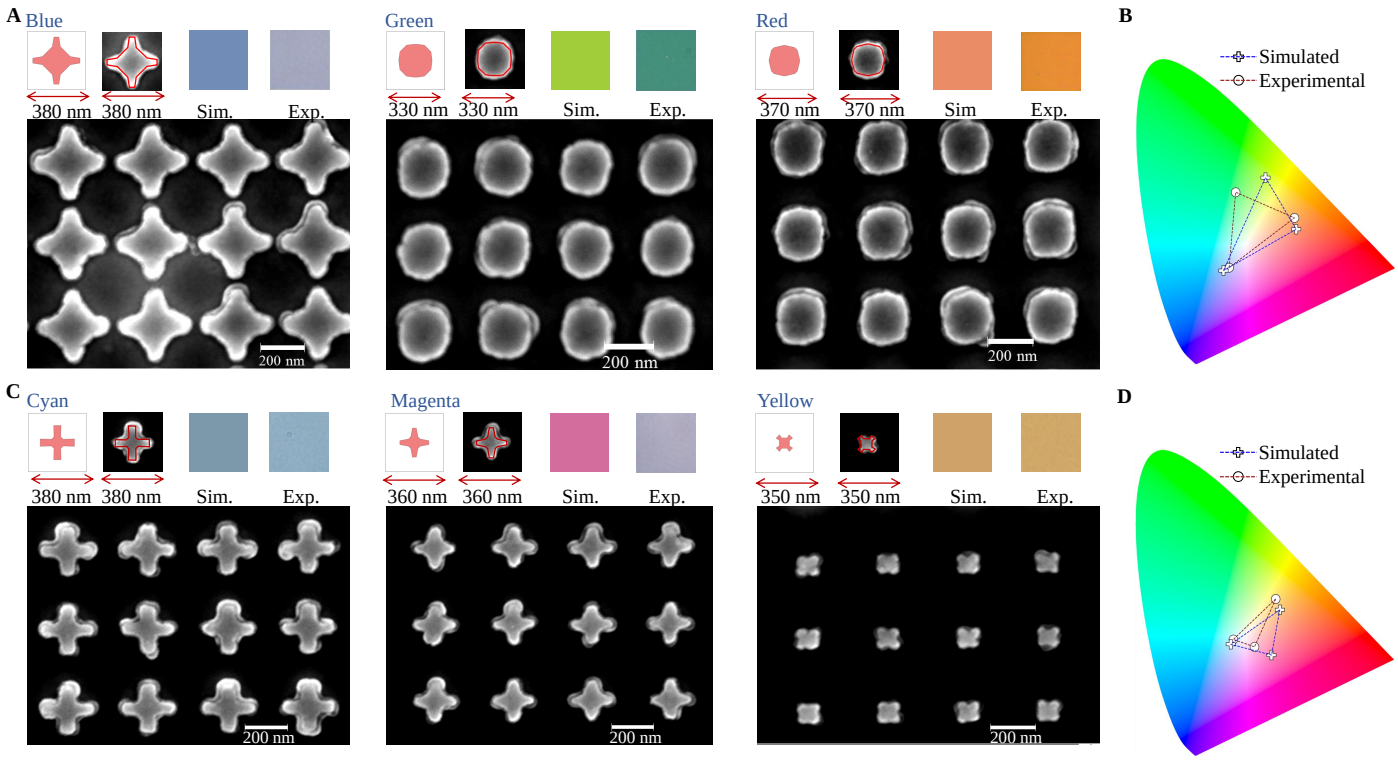

Fig. S-5. SEM and Optical micrographs of RGB and CMY color filters. **A,C:** For all CFAs, theoretical designs are compared with the SEM micrographs of fabricated structures. The simulated (calculated from transmission spectra) and experimental (obtained from optical characterization) are also compared. **B,D:** The simulated and experimental RGB and CMY color gamuts are compared in a CIE-1931 chromaticity diagram.

In order to demonstrate the efficacy of proposed polygonal encoding and the learning ability of DNN for such encoding, we have considered the example of 7-sided asymmetric polygonal metasurfaces. For such geometry, the 'input' to the DNN is a 15 dimensional parameter vector. The output is the transmittance and reflectance spectra for s-polarized incidence. The network was trained with a training dataset of size 100K. The predicted spectra given by the learned model are compared with the actual spectra and the results are demonstrated in **figure S-3**. A great deal of similarity can be observed between the predicted and actual spectra, suggesting good prediction capability of the DNN model.

REFERENCES

1. S. S. Panda, H. S. Vyas, and R. S. Hegde, Opt. Mater. Express **10**, 3145 (2020).
2. V. Liu and S. Fan, Comput. Phys. Commun. **183**, 2233 (2012).
3. R. Storn and K. Price, J. global optimization **11**, 341 (1997).
4. P. Rocca, G. Oliveri, and A. Massa, IEEE Antennas Propag. Mag. **53**, 38 (2011).

FULL REFERENCES

1. S. S. Panda, H. S. Vyas, and R. S. Hegde, "Robust inverse design of all-dielectric metasurface transmission-mode color filters," Opt. Mater. Express **10**, 3145–3159 (2020).
2. V. Liu and S. Fan, "S4: A free electromagnetic solver for layered periodic structures," Comput. Phys. Commun. **183**, 2233–2244 (2012).
3. R. Storn and K. Price, "Differential evolution–a simple and efficient heuristic for global optimization over continuous spaces," J. global optimization **11**, 341–359 (1997).
4. P. Rocca, G. Oliveri, and A. Massa, "Differential evolution as applied to electromagnetics," IEEE Antennas Propag. Mag. **53**, 38–49 (2011).